This is an open access article published under an ACS AuthorChoice License, which permits copying and redistribution of the article or any adaptations for non-commercial purposes.

JACS
JOURNAL OF THE AMERICAN CHEMICAL SOCIETY
Article
pubs.acs.org/JACS

Asymmetric Synthesis of Rauhut–Currier type Products by a Regioselective Mukaiyama Reaction under Bifunctional Catalysis

María Frias,[†] Rubén Mas-Ballesté,[‡] Saira Arias,[§] Cuauhtemoc Alvarado,[§] and José Alemán*[,†]

[†]Department of Organic Chemistry (module 01), Universidad Autónoma de Madrid, Cantoblanco, 28049 Madrid, Spain
[‡]Department of Inorganic Chemistry (module 07), Universidad Autónoma de Madrid, 28049 Madrid, Spain
[§]División Académica de Ciencias Básicas, Universidad Juárez Autónoma de Tabasco, 86040 Villahermosa, Tabasco, Mexico

Supporting Information

ABSTRACT: The reactivity and the regioselective functionalization of silyl–diene enol ethers under a bifunctional organocatalyst provokes a dramatic change in the regioselectivity, from the 1,5- to the 1,3-functionalization. This variation makes possible the 1,3-addition of silyl–dienol ethers to nitroalkenes, giving access to the synthesis of tri- and tetrasubstituted double bonds in Rauhut–Currier type products. The process takes place under smooth conditions, nonanionic conditions, and with a high enantiomeric excess. A rational mechanistic pathway is presented based on DFT and mechanistic experiments.

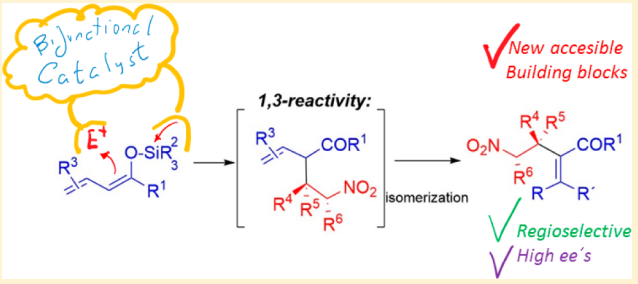

1. INTRODUCTION

In the organocatalytic field, the limited number of activation methods for the preparation of different and novel asymmetric molecules has long impeded their expansion in organic synthesis.[1] This outlook is changing rapidly, and the development of modern organocatalysts has contributed to the emergence of new activation modes. The low price, low toxicity, and unique reactivity of these catalysts make these processes particularly attractive. Despite vast efforts in this area, the development of new bifunctional organocatalysts, such as thiourea[2,3] or squaramide[4] derivatives, is still very limited.[5] The development of new reactions under bifunctional organocatalysts that could increase the number of different activations, and therefore the synthesis of valuable enantioenriched molecules, would be highly desirable. However, most bifunctional catalysts are based on the combination of a Brønsted acid and a Brønsted base (left, Figure 1).

Anionic compounds such as fluoride anions and alkoxides are the most common reagents for the activation of silyl reagents, which are usually incompatible with epimerizable chiral centers and other functionalities. Mukaiyama's[6] and Deng's[7] groups have described the use of chiral salts (PhO^- and $CF_3CO_2^-$ anions) as catalysts in which the anion attacks the silyl reagent and provokes the desired transformation. In recent years, the use of catalysts based on a neutral (uncharged) coordinate organocatalyst (NCO) which can coordinate with a silyl reagent to form an active complex was developed by Kobayashi and others.[8] Different NCOs such as sulfoxides, phosphine oxides, or amines have been used for the activation of silyl reagents, but never in a bifunctional manner. This reaction is generally limited to the use of allylsilanes, and only an α-attack on C═N and C═O bonds has been achieved. However, the

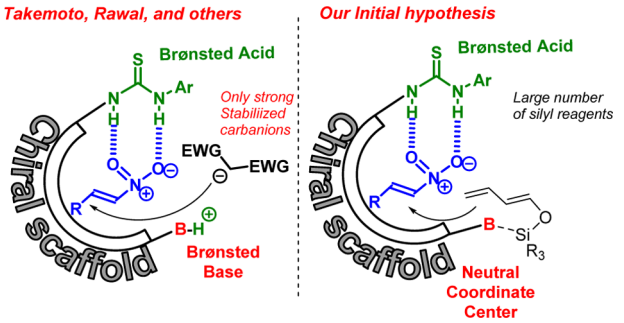

Figure 1. Comparison of the two activation modes of bifunctional catalysts.

application of this NCO to a bifunctional organocatalyst has not yet been applied. This strategy will allow the activation of different electrophiles by the bifunctional catalyst to give the functionalized products together with regeneration of bifunctional neutral coordinate organocatalyst (right, Figure 1). In principle, the use of these bifunctional catalysts would be problematic since the neutral coordinate center (previously used as a Brønsted base) of these species would attack the silyl reagent (forming the covalent bond N^+-SiMe_3) and stop the catalytic cycle (right, Figure 1). However, the development of these processes could provide access to the unknown reactivity of these silyl reagents.

In order to test these initial hypotheses, the addition of the (*Z*)-(buta-1,3-dien-1-yloxy)trimethylsilane **1a** ($R^1 = R^2 = H$) to

Received: July 29, 2016
Published: December 22, 2016

 © 2016 American Chemical Society

DOI: 10.1021/jacs.6b07851
J. Am. Chem. Soc. 2017, 139, 672–679

the nitroalkene **2a** was chosen as a model reaction (Scheme 1). Different excellent and brilliant asymmetric metal catalyzed

Scheme 1. Comparison of the Known Asymmetric Reactivity of 1,5-Mukaiyama Silylenolates with the Present Work

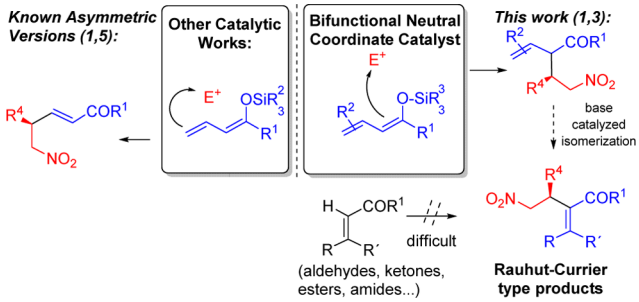

examples from Denmark's,[9] Katsuki's,[10] Campagne's,[11] Evans's,[12] and Carreira's[13] groups among others,[14] as well as the organocatalytic examples from Schneider,[15] Kalesse,[16] List,[17] and Deng,[7] have shown that the most reactive position of the formal dienolate (**1a**) is the remote C5-position (left, Scheme 1).[18] The orbital coefficients and electrophilic susceptibility are mainly responsible for this reactivity,[18a] provoking the observed 1,5 nucleophilic attack. It would be highly desirable if a catalyst could change to the 1,3-selectivity. In addition, the double bond of the intermediate obtained would be isomerized and result in Rauhut–Currier type products, which are excellent building blocks for the synthesis of complex molecules (right, Scheme 1).[19] The lack of reactivity of the mono-β-substituted and β,β-disubstituted double bonds makes difficult the synthesis of these enantioenriched tri- and tetrasubstituted double bonds with different electron withdrawing groups in the Rauhut–Currier reaction (bottom right). In this work, for the first time, the addition of silyl dienol ethers to nitroalkenes, catalyzed by bifunctional catalysts, to obtain any kind of Rauhut–Currier products with high ee's is achieved. In addition, a rational mechanistic pathway based on DFT and mechanistic experiments are presented.

2. RESULTS AND DISCUSSION

2.1. Screening and Scope. Our screening started with the trimethylsilane derivative **1a** and nitrostyrene **2a** in the presence of 20 mol % of the cinchona thiourea catalyst **4a** (entry 1, Table 1). Surprisingly and by contrast with the previous catalytic results reported in the literature,[9−17] only the 1,3 nucleophilic attack product (**3a**) was observed with a low conversion (20%) and moderate enantiomeric excess (50%). Other thiourea cinchona catalysts **4b,c** gave similar conversions with slightly better ee's in the case of the catalyst **4b** (entries 2−4). Driven by our experience in bifunctional catalysis,[20] we decided to explore Takemoto's (**4e**) and Rawal's catalysts (**4f**) (entries 5 and 6). We found a similar result with **4e** to those obtained previously with **4a−d** (ee = 56%, entry 5). However, a better enantiomeric excess (ee = 81%) was found with the squaramide **4f** (entry 6). In the next step we explored different solvents under **4f** catalysis. Interestingly, the use of dry xylene did not result in any conversion at all, whereas other bench solvents, such as THF and DCE, promoted the reaction from low to moderate conversion (entries 7−9). However, the addition of 5 equiv of water increased the conversion (entries, 10−12, see Supporting Information for the full study),

Table 1. Optimization of the Rauhut−Currier Reaction under Squaramide and Thiourea Catalysis[a]

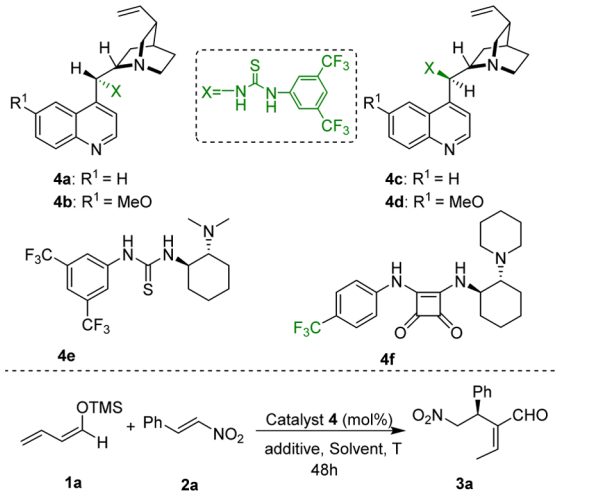

entry	catalyst (mol %)	solvent, additive	ee (%)	convrsn[b] (%)
1	**4a** (20 mol %)	CH_2Cl_2	50	21
2	**4b** (20 mol %)	CH_2Cl_2	67	10
3	**4c** (20 mol %)	CH_2Cl_2	56	30
4	**4d** (20 mol %)	CH_2Cl_2	64	20
5	**4e** (20 mol %)	CH_2Cl_2	56	55
6	**4f** (20 mol %)	CH_2Cl_2	81	48
7	**4f** (20 mol %)	dry xylene		nr
8	**4f** (20 mol %)	THF	96	22
9	**4f** (20 mol %)	DCE	99	63
10	**4f** (20 mol %)	xylene + H_2O[c]	96	69
11	**4f** (20 mol %)	Tol + H_2O[c]	96	88
12	**4f** (20 mol %)	DCE + H_2O[c]	>99	100
13	**4f** (10 mol %)	DCE + H_2O[c]	>99	100 (86)[d]
14	**4f** (5 mol %)	DCE + H_2O[c]	97	53

[a]Conditions: **1a** (0.3 mmol), **2a** (0.1 mmol), catalyst (mol %) in the solvent indicated (0.3 mL) at rt and stopped at 48 h. [b]Conversion measured by ^{1}H NMR. [c]5.0 equiv of H_2O was used as an additive. [d]Isolated yield in parentheses.

remaining equal to or similar in enantioselectivity. In the case of DCE a conversion of >99% and >99% ee was found (entry 12). Then lower catalytic loadings were studied; these also produced a similar result with 10 mol % catalyst **4f** (entry 13), but 5 mol % provoked a substantial decrease in the final conversion (entry 14). The squaramide **4f** showed higher rigidity and increased H-bond distance and canted H-bond angle than thioureas,[4b] offering a higher enantioselectivity in this reaction.

Under these optimized conditions, the scope of the reaction using different substituted nitroalkenes **2** and silyl reagents **1** was carried out (Table 2 and Scheme 2). Different electron donating (*p*-MeO, *p*-Me, **3b**, **3c**) or electron withdrawing groups (*p*-F, *p*-CN, **3d**, **3e**) as well as *ortho*-substituent groups (*o*-Cl, **3f**) at the aryl group of the nitroalkene were tolerated under these conditions. Other synthetically useful halogens such as *p*-Br or 3,4-dichloro (**3g**, **3h**) were also studied, and also showed excellent enantioselectivies and diastereoselectivities (only one double bond stereoisomer was found in all these cases). Very interestingly, an alkene containing a boronic acid (**2l**), with acid protons that would interact with the catalytic system, was also compatible, giving the final Rauhut−Currier product **3l** with 99% ee and 71% yield. Heterocycles, double

DOI: 10.1021/jacs.6b07851
J. Am. Chem. Soc. 2017, 139, 672−679

Table 2. Scope of the Rauhut–Currier Reaction under bifunctional neutral squaramide organocatalysis.[a,b]

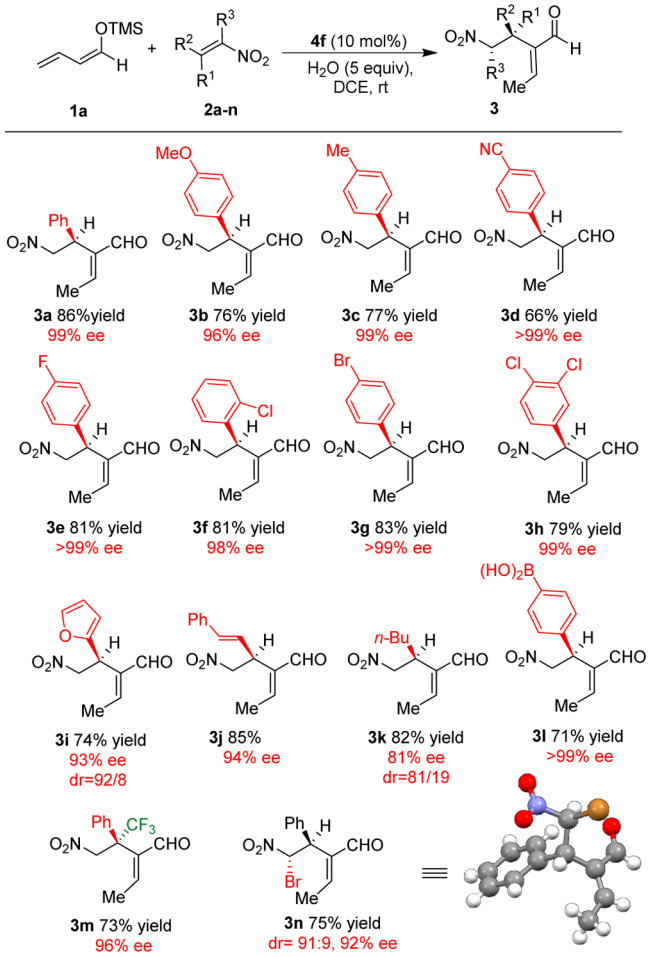

[a]Conditions: **1** (0.3 mmol), **2** (0.1 mmol), **4f** (10 mol %), and H_2O (5 equiv) in DCE (0.3 mL) at rt for 24–48 h. [b]Conversion measured by ^1H NMR.

bonds, and alkyl chains (**3i**, **3j**, **3k**) also worked with excellent yields and good ee's in all cases, but with a lower diastereoselectivity for compounds **3i** and **3k**. The more challenging reactions with trisubstituted nitroalkenes **2m** and **2n** were also studied. The optically enriched quaternary center product **3m** was obtained with a good yield and excellent enantioselectivity (96% ee), whereas the reaction with **2n** gave the final product **3n** with an excellent ee and good diastereocontrol at the bromo position (dr = 91:9). The absolute configuration of the asymmetric center and the configuration of the double bond of **3n** were unequivocally assigned as (*E*, 1*S*, 2*S*) (bottom, Table 2) by X-ray crystallographic analysis.[21] We assigned the same absolute configuration to all the double enals **3** as *E*, 2*S*.

The substitution at the silyl dienol ether was studied with **1b–f** (Scheme 2). The substitution at the 4- and 5-positions led to the *β*,*β*-disubstituted and *β*-monosubstituted adducts **3o** and **3p** in good yields and enantioselectivities which are not possible to obtain by the reported Rauhut–Currier reactions (equations a and b).[22] In addition, the reaction tolerated different groups in *α* position to the TMSO group at the silylenolate **1d–f**. Therefore, the phenyl group led to the ketone **3q** with an excellent enantioselectivity (equation c) whereas the silyl reagent **1e** reacted with **2o** to give the

Scheme 2. Different Substitution and Functional Groups at the Double Bond of the Silyl Dienolate

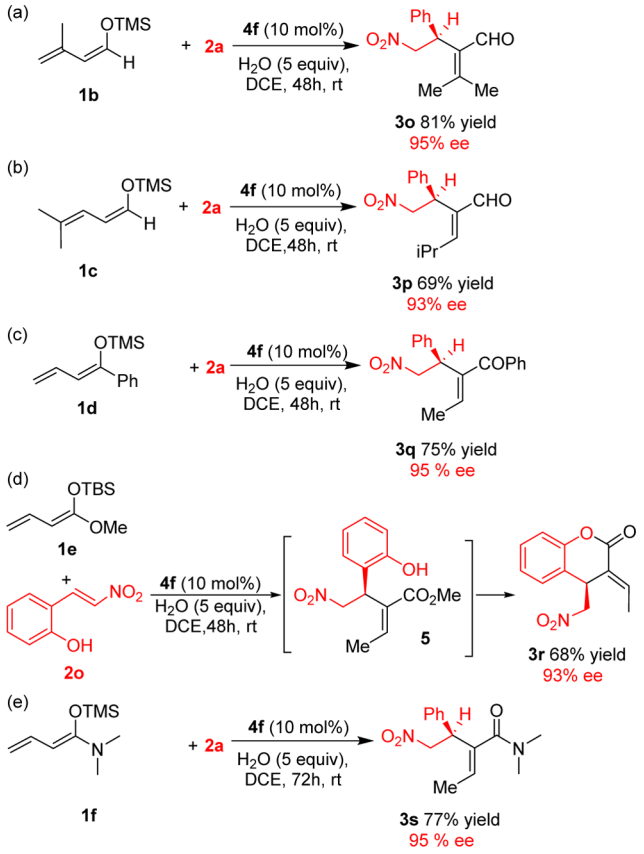

intermediate **5**, which spontaneously cyclized under the basic conditions to give the final lactone **3r** with a good ee and yield (equation d). Finally, the synthesis of amides, which cannot be activated under the standard Rauhut–Currier reaction, gave the adduct **3s** in an excellent yield and enantioselectivity (equation e).

The Rauhut–Currier products obtained can be selectively reduced to obtain precursors of important amino acids, which are analogues of important pharmaceutical products.[23] The products **3a** and **3b** were reduced with Zn in an acidic medium to produce the amino alcohols **7a** and **7b** with good enantioselectivity (left, Scheme 3). In addition, the pyrrolidine **6a** was obtained with excellent ee when H_2 under a palladium catalyst was used (right, Scheme 3).

Scheme 3. Derivatization of Rauhut–Currier Adducts

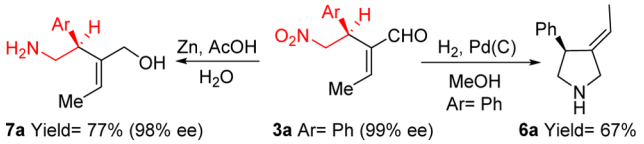

2.2. Mechanism Proposal. A fascinating feature of the results reported herein is the functionalization of the C-3 carbon instead of the C-5 of the silyl dienol ether **1**, even though the latter is significantly the most nucleophilic (Scheme 1). By contrast, in all the reported systems, the functionalization of the C-5 instead of the C-3 has been observed.[9−17] Indeed, a natural population charge analysis of the silyl dienol

DOI: 10.1021/jacs.6b07851
J. Am. Chem. Soc. 2017, 139, 672–679

ether **1a**, by means of DFT calculations, indicates a higher negative charge in C-5 than in C-3 (see Supporting Information for further details). Therefore, the bifunctional catalyst should in some way direct the reactivity of substrates (**1** and **2**) toward this unprecedented reactivity. In order to understand how a bifunctional organocatalyst works, numerous experimental evidence has been collected, which oriented further DFT calculations on the catalytic mechanism.

Water Role. First, we mixed a stoichiometric amount of the catalyst **4f** and TMSCl, obtaining a new silylated species (**4f-Cl**, Scheme 4) that contained the N^+−TMS adduct and a chloride

Scheme 4. NMR Studies in the Silylation of the Squaramide Catalyst 4f

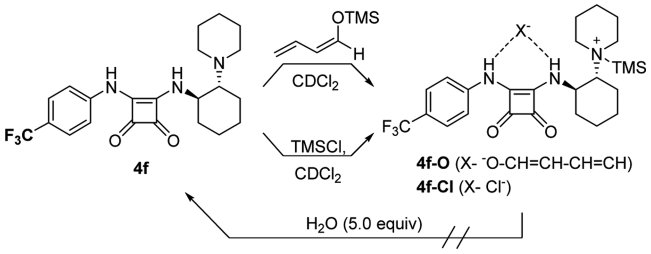

anion stabilized by hydrogen bonding (N−H···Cl^-···H−N), which was confirmed by comparison of ^{1}H NMR and ^{13}C NMR of the initial **4f** catalyst with the **4f-Cl**. In addition, this structure was also established by 2D-HMBC{^{1}H,^{29}Si}, where a ^{29}Si chemical shift at 7.33 ppm, according to a Si−N bond,[24] was found (see Supporting Information for details). In parallel, a mixture of **4f** and silyl dienol ether **1A** led to a similar species (**4f-O**), which also contained an ammonium adduct (N^+−TMS) and, instead of a chloride anion, contained the dienolate fragment, establishing hydrogen bonding between the two NH protons of squaramide and dienolate anion (see Supporting Information). However, the addition of 5 equiv of water did not affect **4f-Cl** or **4f-O**, after some hours, even when solutions were heated.

In addition, we carried out the NMR titration of catalyst **4f** (host) and silyl dienol ether **2a** (guest) in the presence and absence of water (see Supporting Information). Without water, a new silylated species is formed (**4f-O**), confirmed by 2D-HMBC{^{1}H,^{29}Si}, where a new ^{29}Si chemical shift at 7.33 ppm appeared. This is in accordance with a Si−N bond which is identical to the one obtained by direct silylation with TMS-Cl (**4f-Cl**). However, when water was present in the reaction medium, silylation of the catalyst **4f** was not observed by 2D-HMBC{^{1}H,^{29}Si}. Therefore, water is preventing the dead-end of the catalytic cycle and favoring the observed reactivity.

Two important hints can be extrapolated from these results: First, the activation of the reagent **1a** should not proceed by direct interaction with the amine of the bifunctional catalyst **4f**, because the N^+−TMS adduct is unreactive to hydrolysis. Therefore, the **4f-O** species are a dead-end in the catalytic cycle. Second, the anion binding of the squaramide moiety[25] with the oxygen anion (N−H···$^-$O(C_4H_5)···H−N) indicates that the catalytic cycle can be initiated by a species in which the silyl dienol ether **1A** is coordinated to the squaramide fragment, instead of the proposal in which the nitro group is stabilized by a hydrogen bond interaction (as in Takemoto's model[26]).

In a subsequent series of experiments, it was determined that 5 equiv of water was required to obtain good yields (see Supporting Information). This observation suggests that the activation of reagent **1a** proceeds via hydrolysis. In fact, the KIE value of 2.2, measured by comparing the initial rates of reaction in the presence of either H_2O or D_2O, indicates that the hydrolysis of silyl dienol ether is involved in the rate-determining step (see Supporting Information).

Hydrogen Bond Coordination. Combining all the experimental evidence presented above, we carried out a series of DFT calculations[27] in order to define a plausible pathway that could explain all the results obtained. Regarding the squaramide bifunctional catalyst we considered a simplified structure, in which the CF_3 group in the benzene ring was substituted by a hydrogen atom and the six-membered ring cycle NC_5H_{10} was modeled as $N(CH_3)_2$. Such simplifications decreased the computational costs by decreasing the number of basis functions and avoiding dealing with conformational equilibrium in the NC_5H_{10} ring. In order to validate this approximation, the catalytic activity of a simplified bifunctional catalyst (Ph, and NMe_2 derivative) has been experimentally tested, leading to **3a** as a product with a slightly lower enantioselectivity (ee = 93%) and conversion (90%) than when **4f** was used.

First, in order to determine the most feasible initial species, the equilibrium shown in Scheme 5 was calculated. In

Scheme 5. DFT Studies in the Equilibrium between 1a and 2a with the Squaramide Catalyst

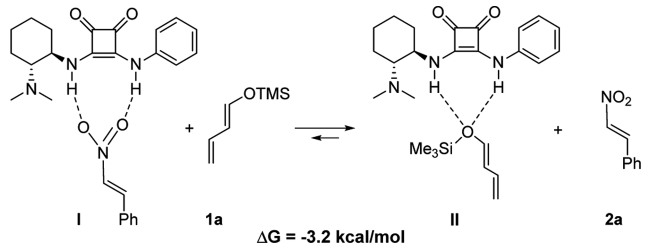

accordance with the experimental observations, coordination to squaramide is more favorable for the silyl dienol ether **1a** than for the nitrostyrene **2a** by 3.2 kcal/mol (**I** versus **II**). Therefore, the process studied is initiated by the hydrolysis step as a consequence of adding a water molecule to species **II** (Scheme 5).

Energetic Profile of the Reaction. In this initial structure (see **III**, Figure 2), a hydrogen bond is found between the water molecule and the amine group (N···H = 1.81 Å). In addition, the oxygen atom of the water molecule is correctly orientated to easily attack the Si center. Further evolution of this system implies at first a proton transfer from the water molecule to the amine nitrogen, followed by a nucleophilic attack of the resulting hydroxide to the silicon atom. In fact, from the starting species **III** to the **IV** there is an energetic cost of 15.5 kcal/mol. In addition, in the potential energy surface, a minimum has been located in which a hypervalent pentacoordinated RO−Si(OH)(CH_3)$_3$ silicon environment is found (structure **IV′**), and formed through the transition state **IV** (Figure 2). However, when thermal corrections are included, the free energy of **IV′** is higher than that of **IV**. Therefore, the process from **III** to **IV′** is probably a barrierless process. Further evolution of such a putative intermediate **IV′** consists of an elongation of the Si−OR bond ($\mathbf{TS_V}$ in Figure 2) that produces the silanol byproduct and the nucleophile [$C_4H_4O^-$]. The later one is stabilized by the hydrogen bonding with the squaramide in a structure very close to the

DOI: 10.1021/jacs.6b07851
J. Am. Chem. Soc. 2017, 139, 672−679

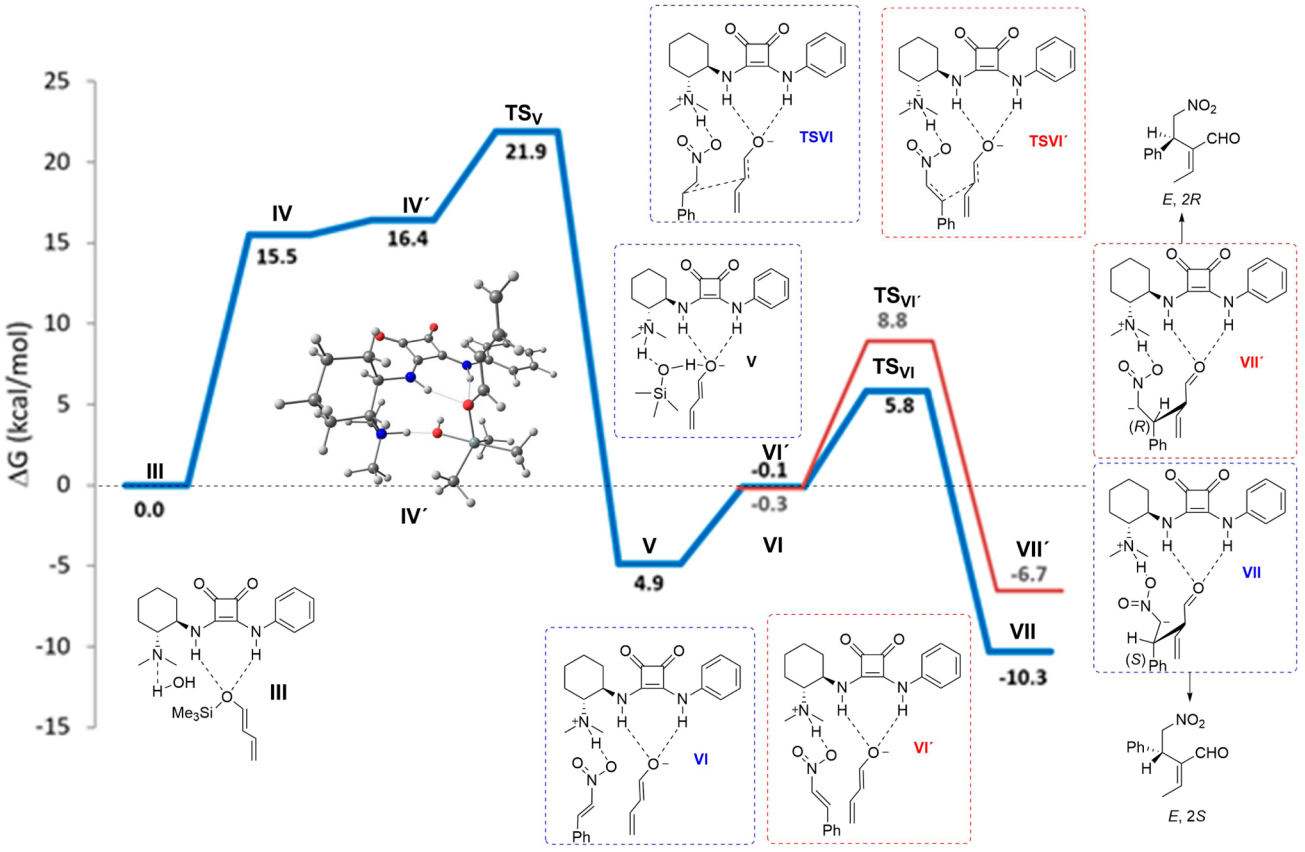

Figure 2. DFT M062x/6-31+G(p,d) reaction energy profile in the addition of **1a** to **2a**.

experimentally detected **4f-O** species. At this point, the hydrolysis step is finished and the C−C bond formation starts. Evolution from **V** to **VI** implies the substitution of silanol by nitrostyrene **2a**, which has an energetic cost of at least 4.7 kcal/mol, due to multiple hydrogen bonding interactions in **V**, in contrast with the simple N−H−ONO(R) interaction found in **VI**. Moreover, this intermediate **VI** is in accordance with the well-known Papai's model.[28] Such preorganization of the two fragments orientates the geometry of the system to specifically generate the new C−C bond (C3 with the Cβ of **2a**), even though C5 is the most nucleophilic site (see top, Figure 3). In addition to the regioselectivity, the enantioselective discrimination in the two different pathways is taking place in this step (**VI** vs **VI′**).

Therefore, the C−C bond formation requires the approach of both C3 and Cβ atoms up to 2.24 and 2.29 Å, which are the distances found in the $\mathbf{TS_{VI}}$ and $\mathbf{TS_{VI}'}$, respectively (Figure 2). Once adduct **VI** and **VI′** are formed, further evolution to form the key C−C bond proceeds through a lower kinetic barrier (5.9 and 9.1 kcal/mol, respectively). As observed in the profile, one enantiomer (**VI**) follows a path with an energy barrier around 3.0 kcal/mol lower than the other one (**VI′**), accounting for the kinetic control responsible for the final enantioselectivity observed. Such energetic differences are related to the geometric constrictions imposed by the relative positions of nitrostyrene and the dienolate nucleophile both fixed by the hydrogen bonding. As a consequence, the hydrogen bonding interaction between dienolate and squaramide is different in **TSVI** and **TSVI′** (for **TSVI**, $d_{O\cdots H}$ = 1.76, 1.90; **TSVI′**, $d_{O\cdots H}$ = 1.92, 1.92, see Figure 3). The lower energy of the fixed conformation of **TSVI** as a result of the bifunctional

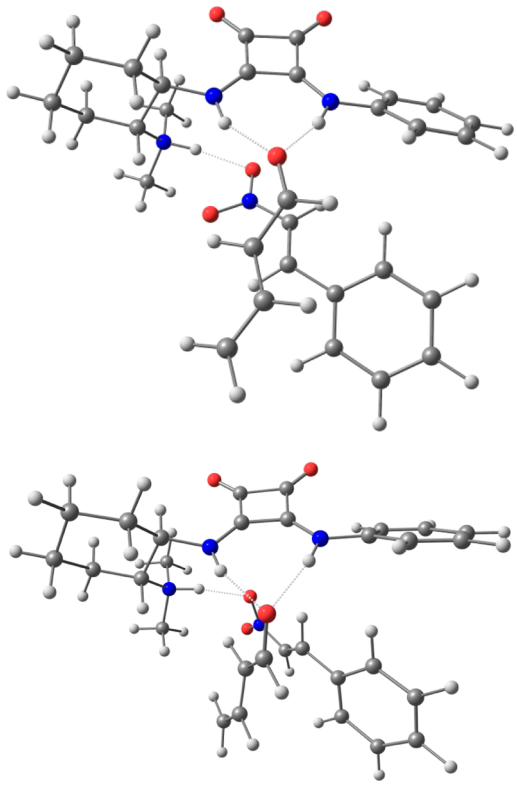

Figure 3. DFT M062x/6-31+G(p,d) of **TSVI** (top) and **TSVI′** (bottom).

DOI: 10.1021/jacs.6b07851
J. Am. Chem. Soc. 2017, 139, 672−679

design of the catalyst is, at the end, responsible not only for the regio- but also for the enantioselectivity (compare **TSVI** and **TSVI′**). Evolution of this transition state results in species **VII** in which the C−C bond is already formed. Species **VII** and **VII′** are very close to the final product **3a** and only differ from it in a proton transfer from the amine N atom of the squaramide to the Cα of the nitronate, followed by a double bond isomerization (bottom and top-right). The double bond isomerization led to the more stable product *E*, which is ∼2 kcal/mol more stable than the *Z* isomer (calculated by DFT, see Supporting Information). Furthermore, the protonation of the nitronate **VII** would also be assisted by the generated silanol from **III** to **VI**.

Alternatively, the coordination of the nitroalkene to the squaramide moiety, following Takemoto's model,[5f] was also considered (see DFT-calculations in Supporting Information). From intermediate **V**, the intramolecular protonation of the enolate with the ammonium fragment occurs without kinetic barrier to give the enol with simultaneous coordination of the nitroalkene to the squaramide (pro-*R* or pro-*S* face, see **VIII** and **VIII′**, see Supporting Information). Although this pathway is also plausible, the kinetic barriers found for the C−C formation in both approaches (**TS-VIII** and **TS-VIII′**) are significantly higher (12.5 and 12.3 kcal/mol) than the approaches shown in Figure 2 (**TSVI** and **TSVI′**, 6.1. and 8.9 kcal/mol).

To understand the energetic differences in **TSVI** and **TSVIII**, an analysis of hydrogen bond distance in the lowest energy transition states for both models has been carried out (Figure 4). A very similar interaction scheme is observed in both cases. In fact, the proton of the enol is completely transferred to the aminic nitrogen in **TSVIII** (1.058 Å, which is comparable to a similar distance in **TSVI**, 1.042 Å). Consequently, an enolate stabilized by hydrogen bonding is found at both transition states (1.759 and 1.903 Å vs 1.748 Å). Therefore, a negative charge is located on the oxygen atom in **TSVIII** as in **TSVI**. The charge distribution (NPA) was in fact analyzed in both **TSVI** and **TSVIII** (see Supporting Information). Based on the collected data, the similarity between these systems from a charge distribution perspective can be verified. For instance, the charge of the oxygen atom in the enolate is −0.76002 for **TSVI** and −0.74707 for **TSVIII**. Moreover, the charge distribution in the newly formed C−C bonds is very similar. Therefore, the activation mode from an electronic point of view is comparable in both models.

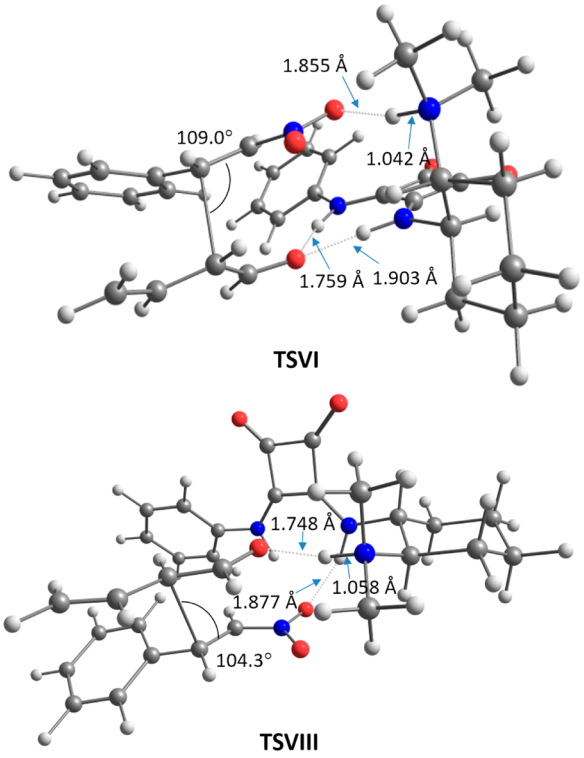

Figure 4. Detailed angles and hydrogen bond distances of **TSVI** (top) and **TSVIII** (bottom).

As the electronic effects are not responsible for the system preference of one model over another, an alternative factor should be claimed. When the structures of both transition states are studied, a more tensioned structure is found for **TSVIII**. Such structural distortion can be described as the deviation of the ideal orientation angle of C−C attack. It is commonly known that the ideal Bürgi−Dunitz angle (BD angle) value is 109°, which is exactly the value found in **TSVI** (see Figure 4). However, in the case of **TSVIII** such value is 104.3°. This distortion implies a subtle energetic cost in the activation barrier in the C−C bond formation. Overall, this phenomenon is a product of the relative orientation of both substrates (nucleophile and electrophile) by hydrogen bond interactions imposed by the bifunctional design of the catalyst.

The high enantio- and regioselectivity and the high reactivity in the activation of the silyl reagent **1** are consequences of the bifunctional structure of catalysts **4**. Therefore, when the same reaction was catalyzed by triethylamine and the monofunctional squaramide **8** (Scheme 6), a very low conversion (15%)[29] and

Scheme 6. System under Two Different Catalysts

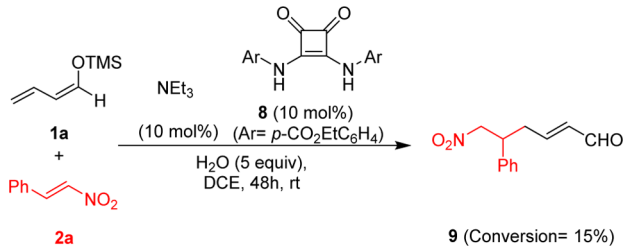

exclusively the 1,5-addition (**9**) were observed in the crude mixture. This is in agreement with all the previous catalytic reports described in the literature,[9−18] which are monofunctional systems and afford only 1,5-addition products. Therefore, our new approach allows a highly enantioselective and 1,3 regioselective functionalization of silyl dienolate derivatives, giving access to Rauhut−Currier products that previously were inaccessible through other methodologies.[19]

3. CONCLUSIONS

In conclusion, we have found that bifunctional catalysts are able to change the reactivity and the regioselectivity of silyl dienol ethers. This provokes a dramatic change in the regioselectivity, from the 1,5- to the 1,3-functionalization, and this variation make possible the 1,3-addition of silyl dienol ethers to nitroalkenes for the synthesis of tri- and tetrasubstituted double bonds in Rauhut−Currier type products. This methodology is compatible with the use of a large variety of nitroalkenes, and different silyl dienol ethers, to give aldehydes, esters, amides, and ketones, Rauhut−Currier products which are not possible

DOI: 10.1021/jacs.6b07851
J. Am. Chem. Soc. 2017, 139, 672−679

to obtain by other methods. The process takes place under smooth and nonanionic conditions with high enantiomeric excess. A rational mechanistic pathway based on DFT and mechanistic studies indicates that the hydrolysis of the silyl dienol ether is the rate-determining step and it is followed by the C−C formation in a regio- and enantioselective manner due to the appropriate orientation of the reagents in the transition state by the bifunctional catalyst.

■ ASSOCIATED CONTENT

Supporting Information

The Supporting Information is available free of charge on the ACS Publications website at DOI: 10.1021/jacs.6b07851.

Experimental procedures, DFT calculations, ^{1}H and ^{13}NMR spectra, and GC and HPLC traces (PDF)

■ AUTHOR INFORMATION

Corresponding Author

*Jose.aleman@uam.es

ORCID

José Alemán: 0000-0003-0164-1777

Notes

The authors declare no competing financial interest.

■ ACKNOWLEDGMENTS

M.F. would like to express thanks to the UAM for a predoctoral fellowship-UAM. Financial support from the Spanish Government (CTQ-2012-12168, CTQ2015-64561-R), European Research Council (ERC-CG, Contract No. 647550), and CONACYT (Programas de redes temáticas: red de investigación en organocatálisis asimétrica 252435) is also gratefully acknowledged. We acknowledge the generous allocation of computing time at the Centro de Computación Científica of the Universidad Autónoma de Madrid (CCC-UAM).

■ REFERENCES

(1) For some selected reviews in organocatalysis, see: (a) Berkessel, A.; Göger, H. *Asymmetric Organocatalysis*; WILEY-VCH: Weinheim, Germany, 2005. (b) Dalko, P. I. *Enantioselective Organocatalysis*; WILEY-VCH: Weinheim, 2007. (c) MacMillan, D. W. C. *Nature* **2008**, *455*, 304. (d) Moyano, A.; Rios, R. *Chem. Rev.* **2011**, *111*, 4703. (e) Bernardi, L.; Fochi, M.; Franchini, M. C.; Ricci, A. *Org. Biomol. Chem.* **2012**, *10*, 2911. (f) Alemán, J.; Cabrera, S. *Chem. Soc. Rev.* **2013**, *42*, 774.

(2) For a deep and pioneering study in H-bonding additives acting as a Lewis acid, see: (a) Schreiner, P. R.; Wittkopp, A. *Org. Lett.* **2002**, *4*, 217. (b) Sigman, M.; Jacobsen, E. N. *J. Am. Chem. Soc.* **1998**, *120*, 4901. (c) Corey, E. J.; Grogan, M. *Org. Lett.* **1999**, *1*, 157. For a review, see: (d) Zhang, Z.; Schreiner, P. R. *Chem. Soc. Rev.* **2009**, *38*, 1187 and references cited therein.

(3) For pioneer work on bifunctional thiourea organocatalyst, see: (a) Okino, T.; Hoashi, Y.; Takemoto, Y. *J. Am. Chem. Soc.* **2003**, *125*, 12672. (b) Okino, T.; Nakamura, S.; Furukawa, T.; Takemoto, Y. *Org. Lett.* **2004**, *6*, 625. For review in thiourea bifunctional catalysts, see (c) Zhang, Z.; Schreiner, P. R. *Chem. Soc. Rev.* **2009**, *38*, 1187. (d) Takemoto, Y. *Chem. Pharm. Bull.* **2010**, *58*, 593.

(4) For pioneering study, see: (a) Malerich, J. P.; Hagihara, K.; Rawal, V. H. *J. Am. Chem. Soc.* **2008**, *130*, 14416. For a review, see: (b) Alemán, J.; Parra, A.; Jiang, H.; Jørgensen, K. A. *Chem. - Eur. J.* **2011**, *17*, 6890.

(5) For reviews in hydrogen bond catalysis, see: (a) Pihko, P. M. *Hydrogen Bonding in Organic Synthesis*; Wiley-VCH Verlag GmbH & Co. KGaA: Weinheim, Germany, 2009. (b) Schreiner, P. R. *Chem. Soc. Rev.* **2003**, *32*, 289. (c) Doyle, A. G.; Jacobsen, E. N. *Chem. Rev.* **2007**, *107*, 5713. (d) McGilvra, J. D.; Gondi, V. D.; Rawal, V. H. In *Enantioselective Organocatalysis*; Dalko, P. I., Ed.; Wiley-VCH: Weinheim, 2007; pp 189−254. (e) Yu, X.; Wang, W. *Chem. - Asian J.* **2008**, *3*, 516. For calculations, see: (f) Okino, T.; Hoashi, Y.; Furukawa, T.; Xu, X. N.; Takemoto, Y. *J. Am. Chem. Soc.* **2005**, *127*, 119.

(6) (a) Nagao, H.; Yamane, Y.; Mukaiyama, T. *Chem. Lett.* **2006**, *35*, 1398. (b) Nagao, H.; Yamane, Y.; Mukaiyama, T. *Chem. Lett.* **2007**, *36*, 666.

(7) Singh, R. P.; Foxman, B. M.; Deng, L. *J. Am. Chem. Soc.* **2010**, *132*, 9558.

(8) For a pioneering work, see: (a) Kobayashi, S.; Nishio, K. *Tetrahedron Lett.* **1993**, *34*, 3453. (b) Kobayashi, S.; Nishio, K. *J. Org. Chem.* **1994**, *59*, 6620. For a review, see: (c) Kobayashi, S.; Sugiura, M.; Ogawa, C. *Adv. Synth. Catal.* **2004**, *346*, 1023 and references cited therein..

(9) (a) Denmark, S. E.; Xie, M. *J. Org. Chem.* **2007**, *72*, 7050. (b) Denmark, S. E.; Beutner, G. L. *J. Am. Chem. Soc.* **2003**, *125*, 7800.

(10) Shimada, Y.; Matsuoka, Y.; Irie, R.; Katsuki, T. *Synlett* **2004**, 57.

(11) (a) Bluet, G.; Campagne, J. M. *Tetrahedron Lett.* **1999**, *40*, 5507. (b) Bluet, G.; Campagne, J. M. *J. Org. Chem.* **2001**, *66*, 4293. (c) Bluet, G.; Bazan-Tejada, B.; Campagne, J. M. *Org. Lett.* **2001**, *3*, 3807.

(12) Evans, D. A.; Hu, E.; Burch, j. D.; Jaeschke, G. *J. Am. Chem. Soc.* **2002**, *124*, 5654.

(13) Pagenkopf, B. L.; Kruger, J.; Stojanovic; Carreira, E. M. *Angew. Chem., Int. Ed.* **1998**, *37*, 3124. (b) Krüger, J.; Carreira, E. M. *J. Am. Chem. Soc.* **1998**, *120*, 837.

(14) (a) Wang, G.; Wang, B.; Qi, S.; Zhao, J.; Zhou, Y.; Qu, J. *Org. Lett.* **2012**, *14*, 2734. (b) Wang, G.; Zhao, J.; Zhou, Y.; Wang, B.; Qu, J. *J. Org. Chem.* **2010**, *75*, 5326. (c) Scettri, A.; Villano, R.; Manzo, P.; Acocella, M. R. *Cent. Eur. J. Chem.* **2012**, *10*, 47. (d) Li, H.; Wu, J. *Org. Lett.* **2015**, *17*, 5424.

(15) Gupta, V.; Sudhir V., S.; Mandal, T.; Schneider, C. *Angew. Chem., Int. Ed.* **2012**, *51*, 12609.

(16) (a) Christmann, M.; Kalesse, M. *Tetrahedron Lett.* **2001**, *42*, 1269. (b) Gieseler, M. T.; Kalesse, M. *Org. Lett.* **2011**, *13*, 2430.

(17) Ratjen, L.; García-García, P.; Lay, F.; Beck, M. E.; List, B. *Angew. Chem., Int. Ed.* **2011**, *50*, 754.

(18) For review of catalytic vinylogous aldol reactions, see: (a) Denmark, S. E.; Heemstra, J. R.; Beutner, G. L. *Angew. Chem., Int. Ed.* **2005**, *44*, 4682. (b) Pansare, S. V.; Paul, E. K. *Chem. - Eur. J.* **2011**, *17*, 8770. (c) Bisai, V. *Synthesis* **2012**, *44*, 1453. For Mannich reactions, see: (d) Schneider, C.; Sickert, M. *Chiral amine synthesis: Methods, developments and applications*; Hugent, T. C., Ed.; Wiley-VCH Verlag: Weinheim, 2010.

(19) For reviews of the Rauhut−Currier reaction, see: (a) Aroyan, C. E.; Dermenci, A.; Miller, S. *Tetrahedron* **2009**, *65*, 4069. (b) Bharadwaj, K. C. *RSC Adv.* **2015**, *5*, 75923. (c) Methot, J. L.; Roush, W. R. *Adv. Synth. Catal.* **2004**, *346*, 1035. (d) Xie, P.; Huang, Y. *Eur. J. Org. Chem.* **2013**, *2013*, 6213.

(20) (a) Jarava-Barrera, C.; Esteban, F.; Navarro-Ranninger, C.; Parra, A.; Alemán, J. *Chem. Commun.* **2013**, *49*, 2001. (b) Parra, A.; Alfaro, R.; Marzo, L.; Moreno-Carrasco, A.; García Ruano, J. L.; Alemán, J. *Chem. Commun.* **2012**, *48*, 9759. (c) Marcos, V.; Alemán, J.; García Ruano, J. L.; Marini, F.; Tiecco, M. *Org. Lett.* **2011**, *13*, 3052.

(21) CCDC 1471840 (**3n**) contains the crystallographic data. These data can be obtained free of charge at www.ccdc.cam.ac.uk.

(22) The Rauhut−Currier reaction works well with β,β-unsubstituted double bonds (see ref 19). Only two asymmetric inter- and intramolecular examples with β,β-unsubstituted α,β-unsaturated double bonds have been recently reported; see: (a) Dong, X.; Liang, L.; Li, E.; Huang, Y. *Angew. Chem., Int. Ed.* **2015**, *54*, 1621. For an intramolecular asymmetric version, see: (b) Zhao, X.; Gong, J.; Yuan, K.; Sha, F.; Wu, X. *Tetrahedron Lett.* **2015**, *56*, 2526.

(23) For references related to the importance of these type of amino alcohols and pyrrolidines, see: (a) Tamura, M.; Tamura, R.; Takeda, Y.; Nakagawa, Y.; Tomishige, K. *Chem. Commun.* **2014**, *50*, 6656. (b) Han, B.; Xiao, Y.; He, Z.; Chen, Y. *Org. Lett.* **2009**, *11*, 4660 and references cited therein..

(24) See: www.pascal-man.com/periodic-table/29Si.pdf.
(25) The coordination of oxygen anions to thiourea or squaramide has been proposed in other works. For reviews in the field, see: (a) Beckendorf, S.; Asmus, S.; García Mancheño, O. *ChemCatChem* **2012**, *4*, 926. (b) Brak, K.; Jacobsen, E. N. *Angew. Chem., Int. Ed.* **2013**, *52*, 534. (c) Phipps, R. J.; Hamilton, G. L.; Toste, F. D. *Nat. Chem.* **2012**, *4*, 603.
(26) Okino, T.; Hoashi, Y.; Furukawa, T.; Xu, X.; Takemoto, Y. *ChemInform* **2005**, DOI: 10.1002/chin.200521034.
(27) Quantum chemistry calculations were carried out using the density functional theory (DFT). In particular, geometry optimizations were performed using the M06-2X functional in combination with the 6-31G+(d,p) basis set including dichloroethane (ε = 10.4) solvent effects with the solvation model density (SMD). For more details see Supporting Information.
(28) Hamza, A.; Schubert, G.; Sóos, T.; Pápai, I. *J. Am. Chem. Soc.* **2006**, *128*, 13151.
(29) In addition, the reaction with Et_3N and squaramide **8** was carried out in two different experiments. A similar conversion (15%) was only found when **8** was used.

DOI: 10.1021/jacs.6b07851
J. Am. Chem. Soc. 2017, 139, 672−679